INTERNATIONAL JOURNAL FOR NUMERICAL METHODS IN ENGINEERING
Int. J. Numer. Meth. Engng 2006; **69**:1–21 *Prepared using* nmeauth.cls *[Version: 2002/09/18 v2.02]*

A bubble-stabilized finite element method for Dirichlet constraints on embedded interfaces

Hashem M. Mourad[1], John Dolbow[1,*], Isaac Harari[2]

[1] *Department of Civil and Environmental Engineering, Duke University, Durham, North Carolina 27708, USA*
[2] *Department of Solid Mechanics, Materials, and Systems, Tel Aviv University, 69978 Ramat Aviv, Israel*

SUMMARY

We examine a bubble-stabilized finite element method for enforcing Dirichlet constraints on embedded interfaces. By embedded we refer to problems of general interest wherein the geometry of the interface is assumed independent of some underlying bulk mesh. As such, the robust imposition of Dirichlet constraints with a Lagrange multiplier field is not trivial. To focus issues, we consider a simple one-sided problem that is representative of a wide class of evolving interface problems. The bulk field is decomposed into coarse and fine scales, giving rise to coarse-scale and fine-scale one-sided sub-problems. The fine-scale solution is approximated with bubble functions, permitting static condensation and giving rise to a stabilized form bearing strong analogy with a classical method. Importantly, the method is simple to implement, readily extends to multiple dimensions, obviates the need to specify any free stabilization parameters, and gives rise to a symmetric, positive-definite system of equations. The performance of the method is then examined through several numerical examples. The accuracy of the Lagrange multiplier is compared to results obtained using a local version of the domain integral method. The variational multiscale approach is shown to both stabilize the Lagrange multiplier and improve the accuracy of the post-processed fluxes.

KEY WORDS: Embedded interface; Lagrange multiplier; finite element; stabilization

1. INTRODUCTION

Recently, much attention has focused on finite element methods employing "embedded" or "immersed" interfaces, i.e. surfaces that aren't fitted or aligned with some underlying bulk mesh. Such techniques aim to circumvent or alleviate the difficulties associated with remeshing the bulk domain as the interface evolves. These methods find application in a wide range of problems of interest to the engineering and materials science communities. For example,

*Correspondence to: John Dolbow, Department of Civil and Environmental Engineering, Duke University, Box 90287, Durham, NC 27708-0287, USA

Contract/grant sponsor: Sandia National Laboratories; contract/grant number: 184592

Received 16 December 2005
Revised 16 December 2005

consider the recent work on fluid-structure interaction [1], cohesive crack growth [2], and sharp phase transitions [3], just to name a few. In this paper, we present a technique that successfully addresses the difficult issue of robustly enforcing Dirichlet constraints on such interfaces. It bears emphasis that our technique is also applicable to "stiff" Neumann constraints, such as those arising from many cohesive models.

For finite element methods that explicitly fit the mesh to the surface of interest, Dirichlet constraints are often enforced through simple collocation at the nodes on the surface. In many cases, this is sufficient to guarantee convergence. For embedded interfaces, however, such a simple approach is not readily available. Most formulations resort to a mixed method, and introduce a Lagrange multiplier to enforce the constraint. Unfortunately, the design of finite-element subspaces for the bulk and Lagrange multiplier fields that satisfy the classical inf-sup condition proposed by Babuška [4] is not a trivial undertaking. The most convenient choice for the discrete subspaces is often one that cannot be guaranteed stable.

In light of these difficulties, Barbosa and Hughes [5] turned to least-squares stabilization as a means of circumventing the inf-sup condition. Stenberg [6] subsequently showed that Nitsche's method, a classical approach for enforcing Dirichlet constraints, could be derived from the stabilized forms proposed by Barbosa and Hughes. Nitsche's method [7] may be viewed as a variationally consistent penalty method, and only requires the specification of a single parameter α to ensure stability. This classical method has garnered much attention of late, for both meshfree methods [8] and finite element methods with embedded interfaces [9]. The issue with Nitsche's method, particularly for evolving interface methods, concerns the practicality of identifying or selecting the stability constant α. Fernandez-Mendez and Huerta [8] proposed solving a local eigenvalue problem to identify the stability constant, but this is not an efficient strategy if required at every time step. Methods that do not rely on the specification of such a parameter are obviously desirable.

Additional emphasis has been placed on this issue by the recent work of Ji and Dolbow [10] and Moës et al. [11] with regard to the eXtended Finite Element Method (X-FEM). The X-FEM is designed to address moving boundary value problems such as crack growth and phase transitions without remeshing. This is effected through a combination of basis enrichment and a separation of computational and physical domains. The origins of the method can be traced back to the work of Belytschko and Black [12] on simulating crack growth with a minimal level of remeshing. Ji and Dolbow showed that for interfacial problems with Dirichlet constraints, the most convenient choice for Lagrange multiplier fields likely violates the inf-sup condition for many choices of enrichment. Moës and coworkers subsequently developed a technique for tailoring a Lagrange multiplier field to the X-FEM. They cited a sensitivity to the stabilization constant in Nitsche's method, and demonstrated that their method is more robust. We note, however, that the method is not straightforward to implement, and further that it remains unclear how to readily adapt the basic construction of their multiplier approximation to three-dimensional problems. Finally, the use of the classical Galerkin formulation to the problem gives rise to a linear algebraic system that is symmetric but *not* positive definite—which precludes the use of some fast and efficient solvers, e.g. conjugate gradient.

In this work, we approach the problem by seeking a suitable enhancement to the bulk field. To fix ideas, we consider a simple one-sided problem involving the Laplace equation for a bulk field on a domain with an embedded interface. The bulk field is specified on the interface through a Dirichlet condition. We decompose the bulk field into coarse and fine scales and introduce a model for the fine-scale field with bubble functions. Such a decomposition is

inspired by the variational multiscale framework developed by Hughes [13, 14], and is related to the class of bubble-stabilized formulations proposed by Brezzi et al. [15] for advection-diffusion. This allows the method to correct for the lack of stability in the standard Galerkin variational formulation of the problem. Upon making particular choices for the finite element approximations to the bulk field and Lagrange multiplier, we show how one can recover a form that is very similar to Nitsche's method. A significant feature of our approach, however, is that it yields an element-level stabilization term α^e that appears naturally via the solution of the fine-scale problem.

The use of element-level bubble functions to stabilize finite element computation originated over twenty years ago (see, e.g., [16]). Bubble-enhanced methods [17], related to stabilized finite element methods [15], are seen as arising from a separation of scales according to the numerical mesh size [18]. Methods such as the residual-free bubbles method [19, 20, 21] (related to the bubble-enriched nearly optimal Petrov-Galerkin method [22]), may be viewed as a localized approach to represent the fine, unresolved, scales, within the variational multiscale framework [13, 14]. A similar result is obtained by employing an element Green's function [13], and the link to residual-free bubbles was explored in [23]. The obvious limitation related to the loss of essential global effects inherent in local approaches may be overcome by employing nonconforming methods [24, 25]. The relationship of variational multiscale methods based on *fine-scale* Green's functions to optimal stabilized methods with global and local character is described in [26].

This paper is outlined as follows. In the next Section, we define the boundary-value problem that will be used to study the proposed method and we provide its standard variational form. In Section 3, the details of the numerical discretization, stabilization with the variational multiscale method, and relationship to Nitsche's method are presented. We also review a recent domain-integral method for computing the interfacial normal flux, considered to be an important quantity of interest for many embedded interface problems. Section 4 provides several numerical examples that illustrate the accuracy and robustness of the proposed method. Finally, we provide a summary and comment on future work in the last section.

2. PROBLEM STATEMENT

Consider the "one-sided problem" described by an interface Γ_* partitioning the domain Ω into the disjoint sets Ω_c and Ω_*, as shown in Figure 1.

Perhaps the simplest one-sided boundary-value problem is given by

$$\Delta u = 0 \qquad \text{in } \Omega_* \tag{1a}$$

$$u = \mathrm{u}_d \qquad \text{on } \Gamma_* \tag{1b}$$

$$\boldsymbol{\nabla} u \cdot \mathbf{n}_\mathrm{o} = \mathrm{h} \qquad \text{on } \Gamma_h \tag{1c}$$

where Δ is the standard Laplace operator, and $\mathbf{n}_\mathrm{o}$ is the outward unit normal to Γ_h, as shown in Figure 1. The above is a simplification of classical one-sided Stefan problems that arise from models for a wide range of evolving interface phenomena. Such models normally include an evolution equation for the geometry of the interface in which the interfacial flux

$$\mathrm{j} = \boldsymbol{\nabla} u \cdot \mathbf{n} \qquad \text{on } \Gamma_* \tag{2}$$

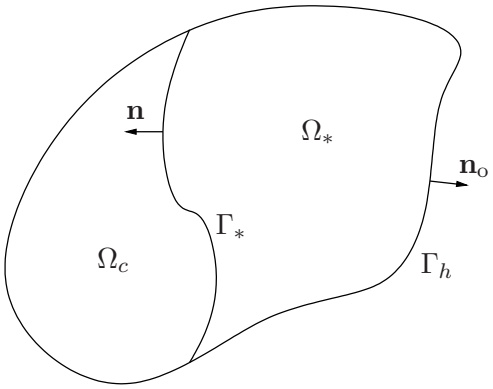

Figure 1. Notation for the one-sided problem. A domain Ω partitioned into regions Ω_c and Ω_* by the interface Γ_*. The normal to the interface, $\mathbf{n}$, is defined such that it points outward from the Ω_* subdomain, as shown.

is a quantity of interest. For example, in many one-sided solidification problems, the normal velocity of the interface is proportional to the interfacial flux.

2.1. Standard weak formulation

We write $\mathcal{S}$ for the space of admissible bulk fields, and $\mathcal{V}$ for the corresponding space of variations. We choose to enforce the constraint (1b) on Γ_* weakly, using a Lagrange multiplier λ belonging to the space $\mathcal{L}$. The weak form reads: Find $(u, \lambda) \in \mathcal{S} \times \mathcal{L}$ such that

$$\int_{\Omega_*} \boldsymbol{\nabla} w \cdot \boldsymbol{\nabla} u \, d\Omega - \int_{\Gamma_*} w\lambda \, d\Gamma = \int_{\Gamma_h} w\mathrm{h} \, d\Gamma \tag{3a}$$

$$-\int_{\Gamma_*} \mu u \, d\Gamma = -\int_{\Gamma_*} \mu \mathrm{u}_d \, d\Gamma \tag{3b}$$

for all $(w, \mu) \in \mathcal{V} \times \mathcal{L}$. The Euler-Lagrange equations associated with this weak form are given by (1) and

$$\lambda = \boldsymbol{\nabla} u \cdot \mathbf{n} \tag{4}$$

3. DISCRETIZATION WITH FINITE ELEMENTS

We consider a quasi-uniform partition Ω^h of the domain Ω into non-overlapping element domains Ω^e with boundaries $\partial\Omega^e$. We assume that the interface Γ_* is approximated with a partition Γ_*^h that has a particular structure; namely, the vertex set for Γ_*^h is taken as the set of intersection points between Γ_* and the set of element edges $\{\partial\Omega^e\}$. We consider an "unfitted" or "embedded" interface method in the sense that no further assumption concerning the structure of the partition Ω^h and the interface partition Γ_*^h is made. For the sake of concreteness, an example of Ω^h and Γ_*^h is shown in Figure 2.

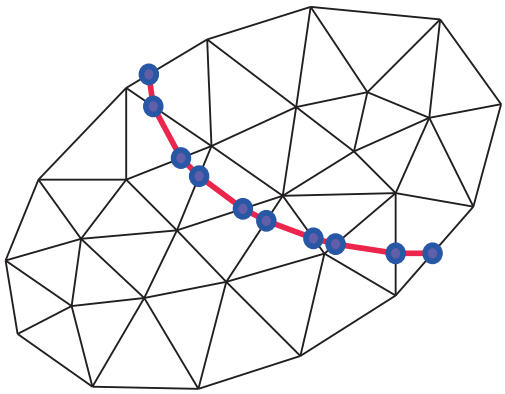

Figure 2. Two-dimensional example of a bulk partition of the domain into a finite element mesh and corresponding partition of the interface. Closed circles represent the vertex set for the interfacial partition.

The difficulties associated with designing finite element subspaces $\mathcal{S}^h \subset \mathcal{S}$ and $\mathcal{L}^h \subset \mathcal{L}$ that satisfy the classical inf-sup condition proposed by Babuška [4] have been examined in several studies; e.g. see Pitkäranta [27], Dahmen and Kunoth [28]. Stabilized methods which can circumvent these difficulties are therefore desirable.

3.1. Stabilization via bubble enrichment

We decompose the approximation u^h to the bulk field u into coarse and fine scales, denoted by

$$u^h(\boldsymbol{x}) = \underbrace{\bar{u}(\boldsymbol{x})}_{coarse} + \underbrace{u'(\boldsymbol{x})}_{fine} \tag{5}$$

and similarly for the weight functions w^h. For the moment, we only assume that the fine-scale functions, u' and w', vanish on the boundary Γ_h. Furthermore, we only consider one scale for the approximate Lagrange multiplier λ^h and its associated weight function μ^h. The Galerkin approximation to (3) thus consists of the coarse-scale equations

$$\sum_e \int_{\Omega_*^e} \boldsymbol{\nabla}\bar{w} \cdot \boldsymbol{\nabla}(\bar{u} + u')\, d\Omega - \sum_e \int_{\Gamma_*^e} \bar{w}\lambda^h \, d\Gamma = \sum_e \int_{\Gamma_h^e} \bar{w}\mathrm{h}\, d\Gamma \tag{6a}$$

$$-\sum_e \int_{\Gamma_*^e} \mu^h(\bar{u} + u')\, d\Gamma = -\sum_e \int_{\Gamma_*^e} \mu^h \mathrm{u}_d \, d\Gamma \tag{6b}$$

and the fine-scale equation

$$\sum_e \int_{\Omega_*^e} \boldsymbol{\nabla}w' \cdot \boldsymbol{\nabla}(\bar{u} + u')\, d\Omega - \sum_e \int_{\Gamma_*^e} w'\lambda^h \, d\Gamma = 0 \tag{6c}$$

where $\Omega_*^e := \Omega^e \cap \Omega_*$ and $\Gamma_*^e := \Gamma_* \cap \Omega^e$.

We now consider an approximation for the coarse scale of the form

$$\bar{u}(\boldsymbol{x}) = \sum_{i \in I} N_i(\boldsymbol{x}) u_i \tag{7a}$$

$$\bar{w}(\boldsymbol{x}) = \sum_{i \in I} N_i(\boldsymbol{x}) w_i \tag{7b}$$

where N_i are the nodal shape functions, and I denotes the set of nodes

$$I = \{ j \,|\, \bar{\omega}_j \cap \Omega_* \neq \varnothing \} \tag{8}$$

which have some portion of their supports ω_j (with closure $\bar{\omega}_j$) intersecting the domain Ω_*. For additional detail and insight into this approach, see Daux et al. [29] and other work on the eXtended Finite Element Method. For the fine-scale approximation, we write

$$u'(\boldsymbol{x}) = \sum_{e \in B} b^e(\boldsymbol{x}) \beta^e \tag{9a}$$

$$w'(\boldsymbol{x}) = \sum_{e \in B} b^e(\boldsymbol{x}) \gamma^e \tag{9b}$$

where b^e denotes the element-level bubble function and B is a subset of the elements in the mesh given by

$$B = \{ s \,|\, \Omega^s \cap \Gamma^h_* \neq \varnothing \} \tag{10}$$

In other words, the fine-scale solution is nonzero only in the interior of elements whose domains intersect the interface. We remark that this restriction is only made for efficiency, and that the developments which follow could just as easily be applied to situations where the fine scale contributes over all of Ω_*.

Substituting (9) into (6c) and invoking the arbitrariness of γ^e leads to an expression of the form

$$\beta^e \int_{\Omega^e_*} \boldsymbol{\nabla} b^e \cdot \boldsymbol{\nabla} b^e \, d\Omega = \int_{\Gamma^e_*} b^e \lambda^h \, d\Gamma - \int_{\Omega^e_*} \boldsymbol{\nabla} b^e \cdot \boldsymbol{\nabla} \bar{u} \, d\Omega \tag{11a}$$

or, equivalently

$$\beta^e \int_{\Omega^e_*} \boldsymbol{\nabla} b^e \cdot \boldsymbol{\nabla} b^e \, d\Omega = \int_{\Gamma^e_*} b^e \left(\lambda^h - \boldsymbol{\nabla} \bar{u} \cdot \mathbf{n} \right) \, d\Gamma + \int_{\Omega^e_*} b^e \Delta \bar{u} \, d\Omega \tag{11b}$$

for each $e \in B$. The above can easily be solved for the element-level fine-scale degrees of freedom β^e in terms of the coarse-scale variables, yielding

$$\beta^e(\bar{u}, \lambda^h) = \frac{\int_{\Gamma^e_*} b^e \left(\lambda^h - \boldsymbol{\nabla} \bar{u} \cdot \mathbf{n} \right) \, d\Gamma + \int_{\Omega^e_*} b^e \Delta \bar{u} \, d\Omega}{\int_{\Omega^e_*} \boldsymbol{\nabla} b^e \cdot \boldsymbol{\nabla} b^e \, d\Omega} \tag{12}$$

It is clear from this expression that the fine scales are driven by the coarse-scale residuals.

Using (9) with the coarse-scale weak form (6a, 6b) we obtain

$$\sum_e \int_{\Omega_*^e} \boldsymbol{\nabla}\bar{w}\cdot\boldsymbol{\nabla}\bar{u}\,d\Omega + \sum_{e\in B}\beta^e\int_{\Omega_*^e}\boldsymbol{\nabla}\bar{w}\cdot\boldsymbol{\nabla}b^e\,d\Omega - \sum_e\int_{\Gamma_*^e}\bar{w}\lambda^h\,d\Gamma = \sum_e\int_{\Gamma_h^e}\bar{w}\mathrm{h}\,d\Gamma \tag{13a}$$

$$-\sum_e\int_{\Gamma_*^e}\mu^h\bar{u}\,d\Gamma - \sum_{e\in B}\beta^e\int_{\Gamma_*^e}\mu^h b^e\,d\Gamma = -\sum_e\int_{\Gamma_*^e}\mu^h\mathrm{u}_d\,d\Gamma \tag{13b}$$

It can be verified, after some algebraic manipulation, that substitution of (12) into (13) leads to a symmetric, positive-definite system of equations. This is a significant advantage over methods that simply attempt to design subspaces $\mathcal{S}^h$ and $\mathcal{L}^h$ such that the standard formulation is BB-stable.

3.2. Relation to Nitsche's method

To show the relationship between this method and the classical one due to Nitsche [7], we now consider a particular choice for the approximate Lagrange multiplier λ^h and coarse-scale bulk field $\bar{u}$. Namely, we consider a piecewise-constant Lagrange multiplier, such that

$$\lambda^h\Big|_{\Gamma_*^e} = \lambda^e \tag{14}$$

and a piecewise-linear coarse-scale field. In this case, the degrees of freedom λ^e can be obtained from (12) and (13b) as

$$\begin{aligned}\lambda^e &= \frac{-\int_{\Gamma_*^e}(\bar{u}-\mathrm{u}_d)\,d\Gamma\int_{\Omega_*^e}\boldsymbol{\nabla}b^e\cdot\boldsymbol{\nabla}b^e\,d\Omega}{\left(\int_{\Gamma_*^e}b^e\,d\Gamma\right)^2} + \frac{\int_{\Gamma_*^e}b^e(\boldsymbol{\nabla}\bar{u}\cdot\mathbf{n})\,d\Gamma - \int_{\Omega_*^e}b^e\Delta\bar{u}\,d\Omega}{\int_{\Gamma_*^e}b^e\,d\Gamma}\\ &= \frac{-\int_{\Gamma_*^e}(\bar{u}-\mathrm{u}_d)\,d\Gamma\int_{\Omega_*^e}\boldsymbol{\nabla}b^e\cdot\boldsymbol{\nabla}b^e\,d\Omega}{\left(\int_{\Gamma_*^e}b^e\,d\Gamma\right)^2} + \boldsymbol{\nabla}\bar{u}\cdot\mathbf{n}^e\end{aligned} \tag{15}$$

where we have used the fact that a piecewise-linear field possesses a constant gradient and a vanishing Laplacian over each element domain. We have also assumed that each interface element Γ_*^e possesses a constant normal vector, denoted by $\mathbf{n}^e$. Combining (12), (13a) and (15), rearranging terms, and performing some additional algebraic manipulations yields

$$\begin{aligned}&\sum_e\int_{\Omega_*^e}\boldsymbol{\nabla}\bar{w}\cdot\boldsymbol{\nabla}\bar{u}\,d\Omega - \sum_{e\in B}\int_{\Gamma_*^e}\bar{w}(\boldsymbol{\nabla}\bar{u}\cdot\mathbf{n}^e)\,d\Gamma - \sum_{e\in B}\int_{\Gamma_*^e}\bar{u}(\boldsymbol{\nabla}\bar{w}\cdot\mathbf{n}^e)\,d\Gamma + \sum_{e\in B}\alpha^e\int_{\Gamma_*^e}\bar{w}\,d\Gamma\int_{\Gamma_*^e}\bar{u}\,d\Gamma\\ &\qquad = \sum_e\int_{\Gamma_h^e}\bar{w}\mathrm{h}\,d\Gamma - \sum_{e\in B}\int_{\Gamma_*^e}\mathrm{u}_d(\boldsymbol{\nabla}\bar{w}\cdot\mathbf{n}^e)\,d\Gamma + \sum_{e\in B}\alpha^e\int_{\Gamma_*^e}\bar{w}\,d\Gamma\int_{\Gamma_*^e}\mathrm{u}_d\,d\Gamma\end{aligned} \tag{16}$$

where the element-level penalty parameter

$$\alpha^e = \frac{\int\limits_{\Omega^e_*} \boldsymbol{\nabla} b^e \cdot \boldsymbol{\nabla} b^e \, d\Omega}{\left(\int\limits_{\Gamma^e_*} b^e \, d\Gamma \right)^2} \tag{17}$$

A relatively straightforward analysis shows that for an element with characteristic linear dimension h, this quantity scales like $1/h$.

Nitsche's method is a classical method for consistently penalizing Dirichlet constraints on a surface. Applied to (1), using piecewise-linear approximations, Nitsche's method gives rise to the Galerkin formulation

$$\begin{aligned} \sum_e \int\limits_{\Omega^e_*} \boldsymbol{\nabla} w \cdot \boldsymbol{\nabla} u \, d\Omega - \sum_{e \in B} \int\limits_{\Gamma^e_*} w(\boldsymbol{\nabla} u \cdot \mathbf{n}^e) \, d\Gamma - \sum_{e \in B} \int\limits_{\Gamma^e_*} u(\boldsymbol{\nabla} w \cdot \mathbf{n}^e) \, d\Gamma + \sum_{e \in B} \alpha \int\limits_{\Gamma^e_*} wu \, d\Gamma \\ = \sum_e \int\limits_{\Gamma^e_h} w \mathrm{h} \, d\Gamma - \sum_{e \in B} \int\limits_{\Gamma^e_*} \mathrm{u}_d (\boldsymbol{\nabla} w \cdot \mathbf{n}^e) \, d\Gamma + \sum_{e \in B} \alpha \int\limits_{\Gamma^e_*} w \mathrm{u}_d \, d\Gamma \end{aligned} \tag{18}$$

where α is a constant parameter. Comparing with (16), the only qualitative differences concern the element penalty parameter α^e instead of a constant global parameter α, and the product of interface integrals versus the integral of a product on the interface. Further, Nitsche [7] showed that α must scale like $1/h$ to guarantee convergence, which appears to be satisfied by (17).

Remarks

1. The element-level parameter α^e follows automatically upon the choice of basis for the fine-scale solution. This is consistent with the application of the variational multiscale method to other classes of boundary-value problems, (e.g. see Masud and Khurram [30] and the references therein).
2. The bubble functions b^e in (9) are typically chosen to vanish on element boundaries $\partial\Omega^e$. Under these conditions, the fine-scale solution does not contribute to the approximation on the interface in the degenerate case when the interface aligns with an element edge. The consequences of this degenerate case are examined in Section 4, but it bears emphasis that nothing in the above derivation specifically requires the use of such bubbles.
3. Numerical quadrature rules must be adjusted for bulk elements that are intersected by the interface such that Ω^e is partitioned between Ω_* and Ω_c, to accurately calculate the contribution of such elements to the matrix system of equations. For details, see Daux et al. [29].

3.3. Choice of bulk and interfacial approximations

We now discuss the specific choices we will consider for the approximations to the coarse and fine scales and the Lagrange multiplier. For simplicity, piecewise-linear Lagrange interpolants are examined for the bulk shape functions N_i in (7). We consider both linear triangular elements and bilinear quadrilaterals.

Polynomial element bubbles are adopted for the fine-scale approximation (9). Specifically, for linear triangular elements, the function

$$b^e = \zeta_1 \, \zeta_2 \, \zeta_3 \tag{19}$$

is used, where ζ_i are the classical triangular (area) coordinates. The bubble function used with bilinear quadrilateral elements is given by

$$b^e = (1-\xi^2)(1-\eta^2) \tag{20}$$

in terms of the natural coordinates ξ and η. It is recognized that these are not necessarily the optimal choices, and that using the optimal bubbles, or good approximations thereof, can greatly improve the effectiveness of the overall stabilization strategy (e.g. see the work of Brezzi and coworkers [17, 31] in the context of advection-diffusion problems).

We consider both piecewise-constant and piecewise-linear (i.e. $\lambda^h \in C^0(\Gamma_*^h)$) approximations to the Lagrange multiplier on Γ_*^h. Practically speaking, discontinuous multipliers are of the greatest interest due to the difficulty of constructing continuous approximations for embedded interfaces in multiple dimensions.

3.4. Domain-integral approximation to the interface flux

In Ji and Dolbow [10], the superconvergent flux projection operator advocated by Carey and coworkers [32, 33] was generalized to embedded interface problems. In essence, this post-processing technique employs the divergence theorem to recast surface-based evaluations into volume (or domain) based evaluations that are better suited for weighted-residual methods.

For each node i whose support ω_i intersects the interface, we first compute

$$\mathrm{j}_i = \frac{1}{\int\limits_{\Gamma_*^e} N_i \, d\Gamma} \sum_e \int\limits_{\Omega_*^e \in \omega_i} \boldsymbol{\nabla} N_i \cdot \boldsymbol{\nabla} u^h \, d\Omega \tag{21}$$

as a projection of the flux over the support of node i, with u^h given by (5). The flux at any point on the interface is then approximated by

$$\mathrm{j}^h(\boldsymbol{x}) = \sum_i N_i(\boldsymbol{x}) \, \mathrm{j}_i \tag{22}$$

In the next section, we will compare the accuracy of this approximation to that of the Lagrange multiplier field on the interface.

4. NUMERICAL STUDIES

Here, we apply the ideas presented above to the following model problem

$$\Delta u = 0 \qquad \text{in } (0,1)\times(\mathrm{y}_*,1) \tag{23a}$$

$$u = \sin(\pi x)\,\hat{v}(\mathrm{y}_*) \qquad \text{at } y = \mathrm{y}_* \tag{23b}$$

$$u = 0 \qquad \text{at } y = 1 \tag{23c}$$

$$\boldsymbol{\nabla} u \cdot \mathbf{n}_{\mathrm{o}} = -\pi\,\hat{v}(y) \qquad \text{at } x = 0,1;\ \mathrm{y}_* < y < 1 \tag{23d}$$

with known analytical solution (see [8, 34]) given by

$$\hat{u}(x,y) = \sin(\pi x)\,\hat{v}(y) \tag{24}$$

where $\hat{v}(\bullet) := \cosh(\pi\bullet) - \coth(\pi)\sinh(\pi\bullet)$. In this two-dimensional problem, the embedded interface Γ_* is a horizontal line located at $y = \mathrm{y}_*$, with $0 \leqslant \mathrm{y}_* < 1$; see Figure 3. We note that

the Dirichlet boundary condition (23c) is enforced by collocation at the nodes lying on the $y = 1$ boundary, i.e. the space $\mathcal{S}^h$ of admissible bulk fields must be chosen such that all $u^h \in \mathcal{S}^h$ satisfy (23c); no Lagrange multipliers are introduced to enforce this boundary condition.

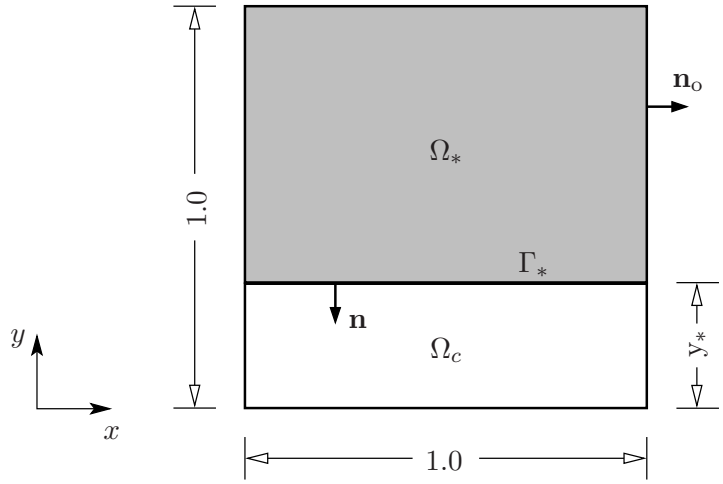

Figure 3. Geometry of the computational domain in the straight-interface model problem.

To evaluate the accuracy in the bulk field, we use the standard L^2 error norm and report normalized, or relative norms. To evaluate the accuracy of the Lagrange multiplier on the interface, we use the normalized error norm

$$\mathcal{E}_d(\lambda^h) := \left(\frac{\int\limits_{\Gamma_*} (\lambda^h - \boldsymbol{\nabla}\hat{u}\cdot\mathbf{n})^2 \, d\Gamma}{\int\limits_{\Gamma_*} (\boldsymbol{\nabla}\hat{u}\cdot\mathbf{n})^2 \, d\Gamma} \right)^{1/2} \tag{25}$$

Where applicable, we also report the error $\mathcal{E}_d(\mathrm{j}^h)$ in the normal flux, j^h, obtained using the domain-integral smoothing technique described in Section 3.4.

4.1. Results obtained on structured grids

The first series of tests is performed using structured grids of linear triangular elements. A typical structured bulk mesh consisting of 32 triangular elements (mesh parameter $h = 1/4$), and the corresponding interfacial mesh are shown in Figure 4. In this case, the interface is located at $\mathrm{y}_* = 1/3$. It is noted that the bottom row of nodes (and elements) do not contribute to the approximation u^h; see Equations (7–10). The second row of nodes from the bottom, however, do contribute to the approximation since their support is partially within Ω_*. The finite-element solution u^h obtained on a more refined mesh ($h = 1/14$) is shown in Figure 5.

To examine the convergence properties of the proposed method, the calculations are carried out on a sequence of four uniform triangular meshes, with decreasing mesh parameter, h. For concreteness, the first two meshes are shown in Figure 6. As can be seen from this figure, the bulk partitions chosen cause the interface to always divide an underlying triangular element into two parts of equal height. We consider the case with the interface located at $y = \mathrm{y}_* = 1/4$.

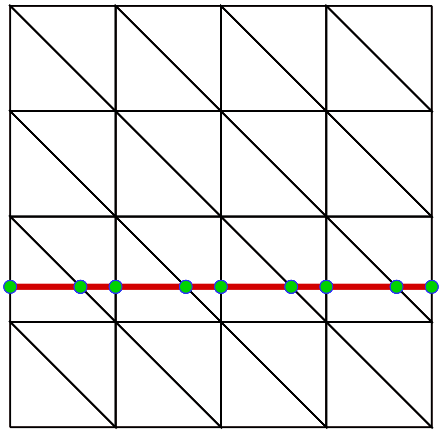

Figure 4. Structured mesh consisting of 32 three-node triangular elements and interfacial mesh with the interface Γ_* located at $y = \mathrm{y}_* = 1/3$.

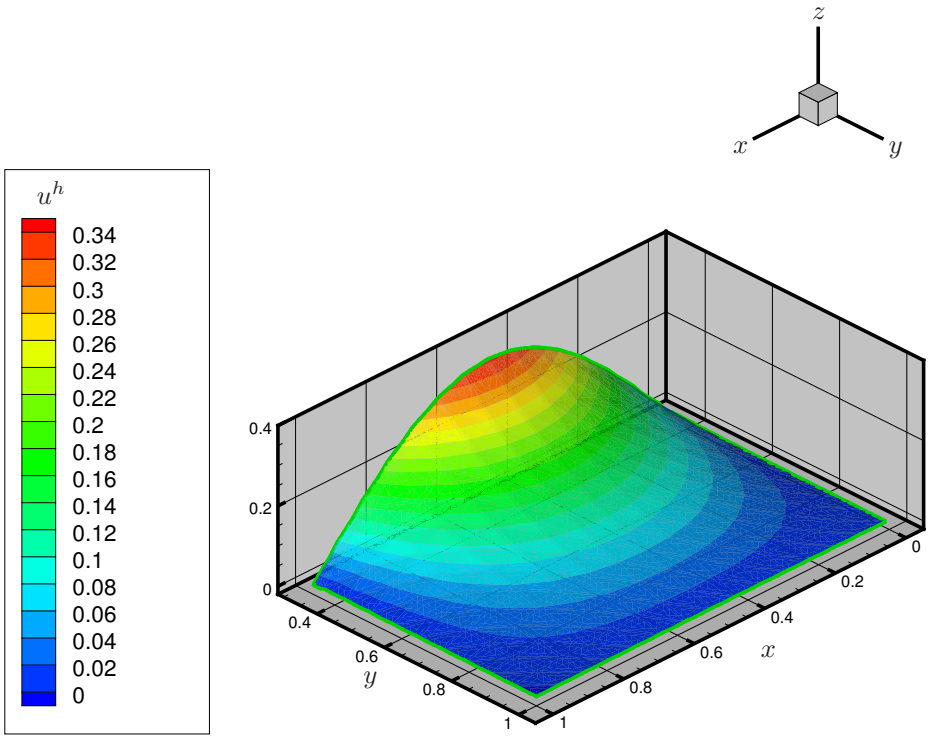

Figure 5. Contour plot of finite-element solution $u^h = \bar{u} + u'$ for the case with $\mathrm{y}_* = 1/3$.

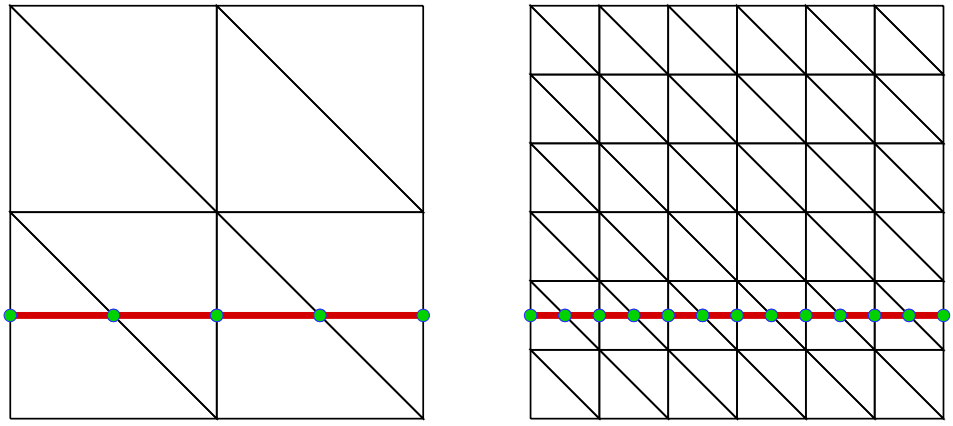

Figure 6. First two structured bulk and interfacial meshes in convergence study.

The errors in the bulk variable and interfacial flux are calculated and plotted against h for each mesh. The results of this convergence study are shown in Figure 7. For the purpose of comparison, convergence results obtained with the standard mixed form (3), i.e. without stabilization, are presented in Figure 8.

With the bubble-stabilized method, we report linear convergence in the Lagrange multiplier and quadratic convergence in the L^2-norm of the bulk field. The rate of convergence in the domain-integral approximation to the interfacial flux is $\mathcal{O}(h^{1.5})$. With the standard mixed method, the error in the Lagrange multiplier increases with mesh refinement, and we note a marked decrease in the accuracy and rate of convergence in the other quantities. While somewhat surprising, piecewise-constant multipliers do appear to give rise to overconstraint for this simple embedded interface problem. This result is consistent with the observations of Moës et al. [11].

Plots of the Lagrange multiplier, λ^h, and the domain-integral approximation to the interfacial flux, j^h, are shown in Figure 9 along with the analytical solution $\boldsymbol{\nabla}\hat{u} \cdot \mathbf{n}$. For comparison, λ^h and j^h, obtained without stabilization, are plotted in Figure 10. Clearly, in this case, large spurious oscillations pollute the Lagrange multiplier solution. This pathology, which is exacerbated by mesh refinement (see Figure 8), is evidently mitigated by the proposed stabilization scheme. It is also clear from the results that the domain-integral approach effectively smoothes the normal gradient of the bulk field on the interface, providing a much more accurate approximation to the interfacial flux than the piecewise-constant Lagrange multiplier.

We also study the sensitivity of λ^h and j^h to the location of the interface relative to the underlying mesh. For this purpose, the distance d between Γ_* and the closest (horizontal) row of nodes is decreased by a factor of 2, starting from $d = h/2$ (the case depicted in Figure 6), down to $d = h/32$. The degenerate case, where the interface coincides with the underlying element edges ($d = 0$), is also considered.

The results of this sensitivity study are presented in Figure 11. For concreteness, d and h are shown for a typical pair of adjacent elements in the inset of Figure 11(a). From these results, it

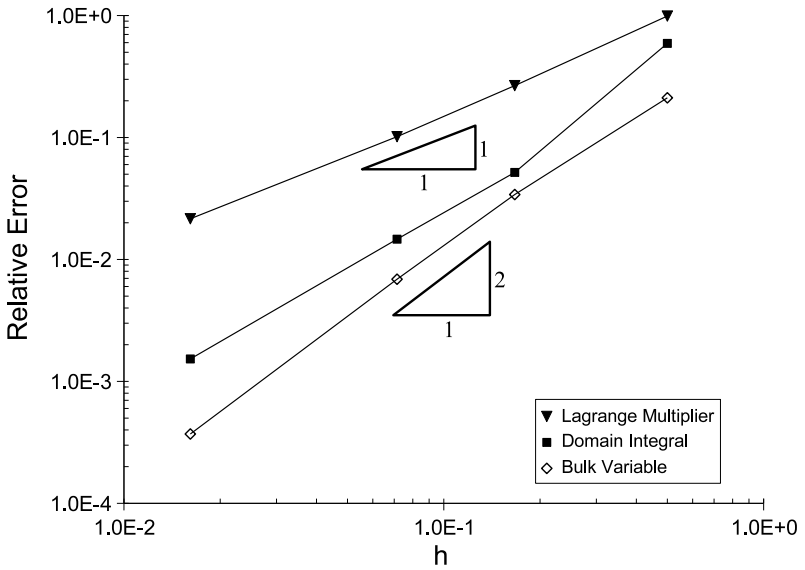

Figure 7. Convergence study results for variational multiscale method on structured triangular grids.

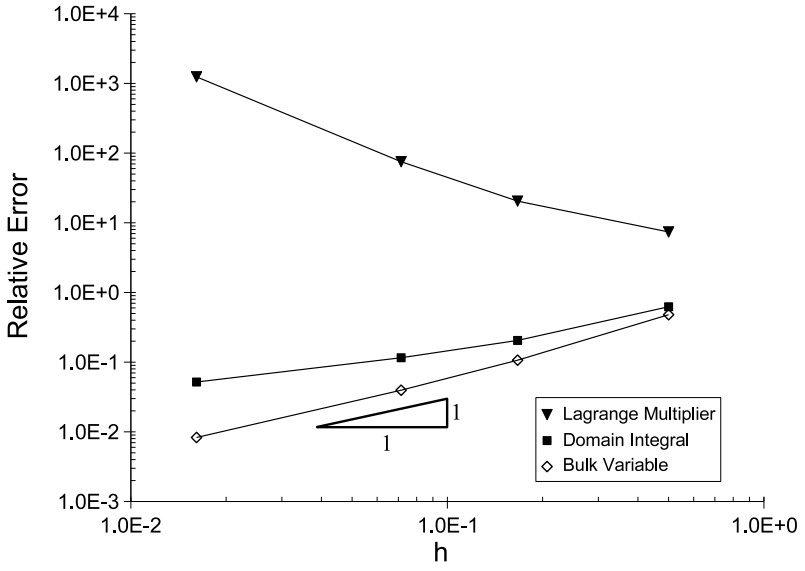

Figure 8. Convergence study results for standard mixed method (without stabilization) on structured triangular grids.

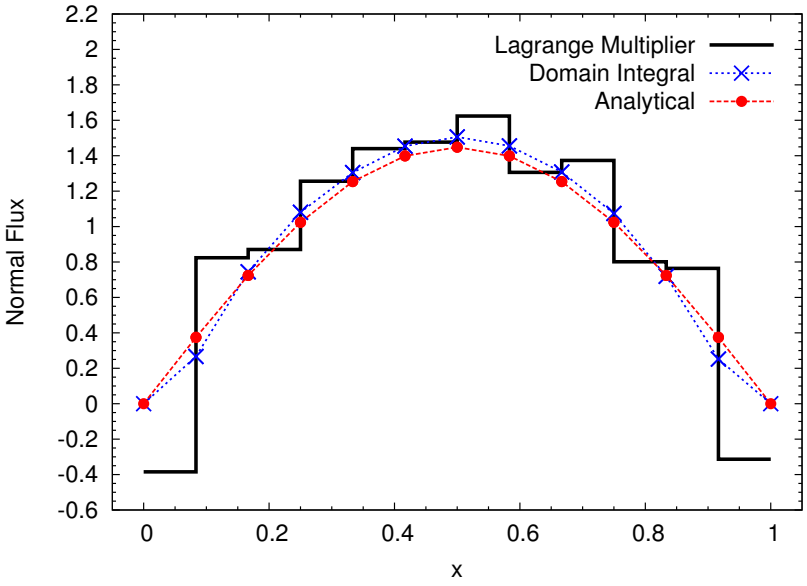

Figure 9. Lagrange multiplier, domain integral, and exact flux on the interface. Results were obtained using a structured triangular mesh.

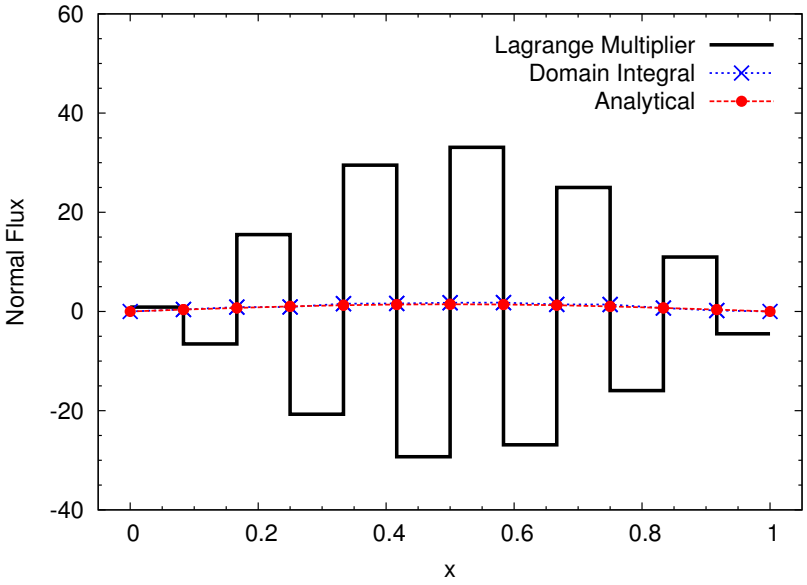

Figure 10. Lagrange multiplier, domain integral, and exact flux on the interface. Results were obtained without stabilization, using a structured triangular mesh.

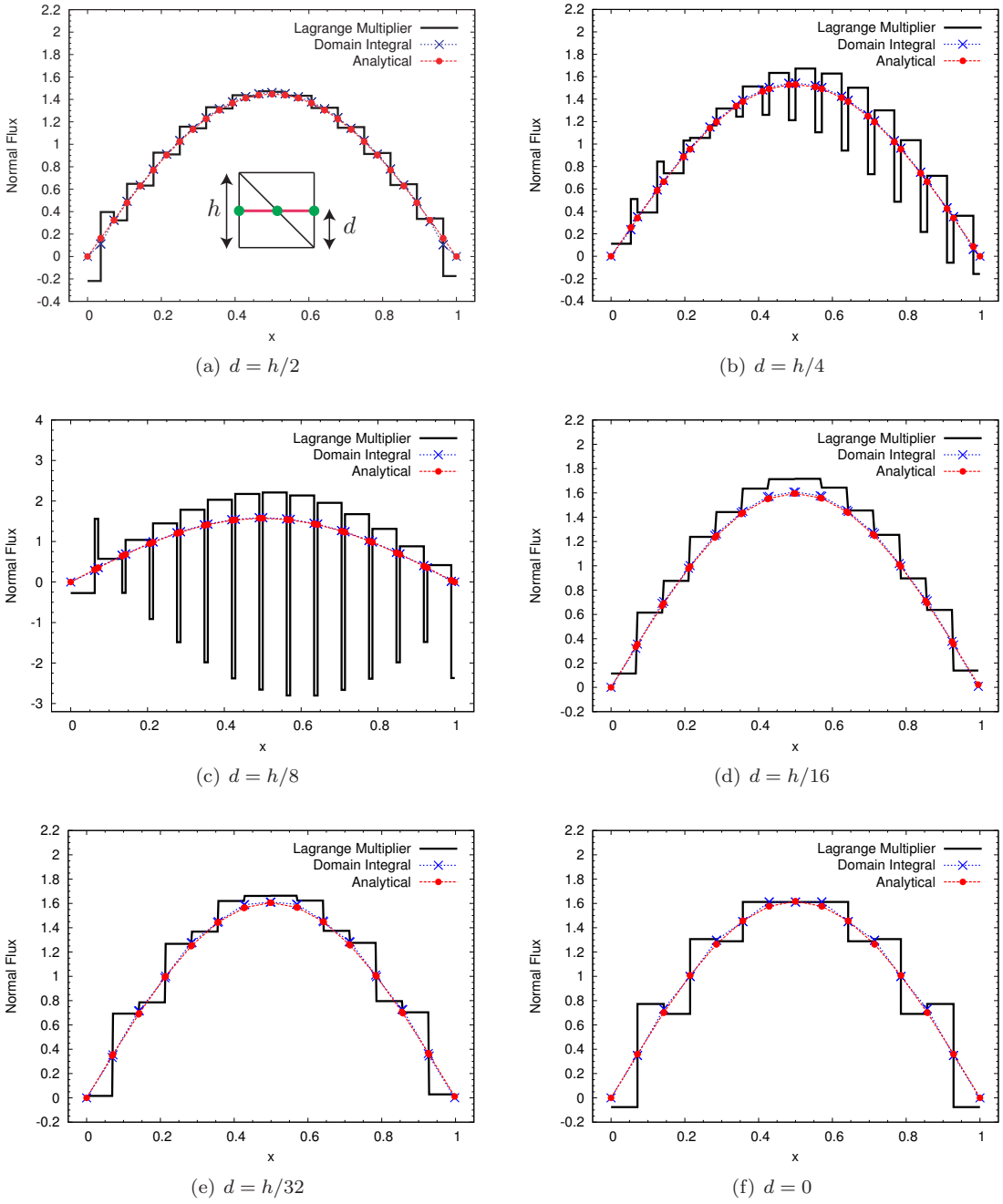

(a) $d = h/2$ (b) $d = h/4$

(c) $d = h/8$ (d) $d = h/16$

(e) $d = h/32$ (f) $d = 0$

Figure 11. Sensitivity of the Lagrange multiplier and domain-integral flux approximation to the location of the interface relative to the mesh. The distance d, between the interface Γ_* and the closest node, varies from (a) $d = h/2$ (see Figure 6) down to (f) $d = 0$ (the degenerate case). The inset in (a) conveys the measures d and h for a typical pair of adjacent elements.

is clear that the domain-integral method yields accurate estimates of the interfacial flux, with all values of d. Conversely, the Lagrange multiplier exhibits a strong sensitivity to the location of the interface. This can be attributed to the following. First, we note that when $d = h/2$, the interface is partitioned into equal segments, each having length $\ell^e := \int_{\Gamma^e_*} d\Gamma = h/2$ (see Figure 6). As d is decreased, the ratio ℓ^e/h approaches zero in some segments (while, in neighboring segments, the same ratio approaches unity). This gives rise to overconstraint, manifested as oscillations in λ^h, which become more pronounced as d becomes smaller, e.g. see Figure 11(c). While these oscillations appear quite large, it should be emphasized that the multiplier obtained with bubble stabilization was nonetheless much more accurate than that obtained without stabilization. Compare these to the results, for example, shown in Figure 10.

It is important to note that, with $d \ll h$, b^e becomes negligibly small on Γ^e_*, and the fine-scale solution vanishes, as implied by Equation (12). In other words, due to its reliance on element bubbles, which vanish on element edges, the proposed stabilized method does not provide an effective remedy for the issue discussed in the previous paragraph. The possibility of making use of edge bubbles to address this issue will be examined in a forthcoming paper. Here, we use a simple heuristic scheme, based on the idea that the Dirichlet constraint need not be enforced on "short" segments, i.e. where ℓ^e/h is smaller than a tolerance value. Such a tolerance is often used with embedded interface methods to determine which elements have been "cut" by the interface. The results shown in Figures 11(d) and 11(e) suggest that this strategy can eliminate overconstraint in some cases. Finally, it is observed that, in the degenerate case itself (Figure 11(f)), λ^h does not exhibit any large spurious oscillations.

4.2. Results obtained on unstructured grids

Consider the unstructured mesh and interface shown on the left in Figure 12. We perform a convergence study by systematically refining this mesh by, effectively, tiling it over the domain as shown on the right of the Figure. What this approach insures, for example, is that if the characteristic mesh size is decreased by some factor, then so too is the dimension of the Lagrange multiplier space increased. This does not necessarily occur if the sequence of meshes are constructed without care.

The convergence results for this case are shown in Figure 13. Comparing these results to those obtained on a sequence of structured grids, we note a slight decrease in the rates of convergence in λ^h and j^h to $\mathcal{O}(h^{0.85})$ and $\mathcal{O}(h^{0.91})$, respectively, as well as a slight decrease in accuracy. The accuracy of the bulk field improves slightly however, and its convergence rate remains quadratic. We note that in each case, the tolerance discussed in the previous section was not invoked. In other words, six multiplier degrees of freedom are associated with the mesh shown on the left in Figure 12, one for each interfacial segment.

4.3. Curved interface

To further study the robustness of the proposed method, we consider the case of a curved interface. Bulk partitions consisting of bilinear quadrilateral elements are used with this model problem, and the accuracy and convergence characteristics are compared to those obtained for the same problem using linear triangular elements. We consider a modified version of (23) as model problem, imposing a Dirichlet boundary condition that is consistent with the solution (24) on a curved interface, in lieu of (23b). Figure 14 shows the interface geometry—a

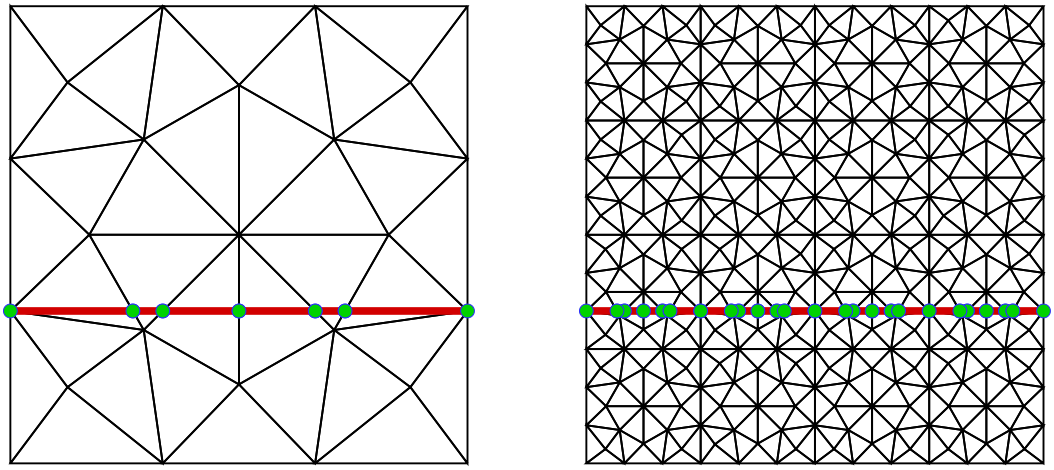

Figure 12. First two unstructured bulk and interfacial meshes in convergence study.

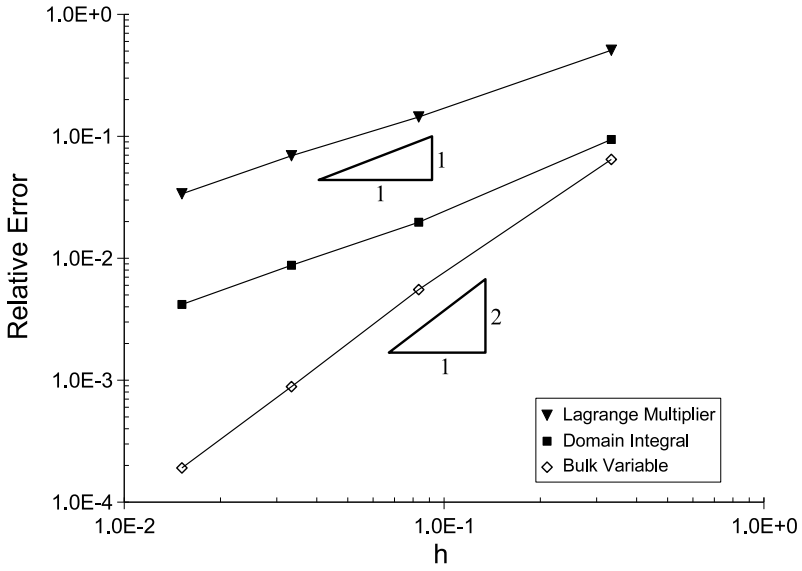

Figure 13. Convergence study results for variational multiscale method on unstructured triangular mesh.

circular arc centered at $(0.5, 1)$, with radius $r = 2/3$—and a typical mesh. A contour plot of the bulk field is shown in Figure 15.

Results pertaining to the spatial convergence of the Lagrange multipliers in this problem are shown in Figure 16. It can be seen from this figure that, in the case of quadrilateral elements, convergence is attained even with the conventional mixed method, and that stabilization does not affect the accuracy or rate of convergence of the results. In the case of triangular elements however, stabilization is clearly needed to attain convergence. It should be noted that in this problem, due to the mismatch between the (circular) interface geometry and the (Cartesian) mesh structure, a reduction in the bulk mesh size, h, does not necessarily cause a comparable reduction in the interfacial mesh size. Consequently, although convergence is achieved, bulk mesh refinement is not necessarily accompanied by a monotonic decrease in the error, as is evident from Figure 16. Regardless, the stabilized results were found to be well behaved for this problem and did not exhibit any spurious oscillations in the multiplier field.

Finally, we did examine the use of piecewise-linear Lagrange multipliers for this problem in conjunction with bilinear quadrilateral elements. In this case, the rate of convergence in the Lagrange multipliers remained at $\mathcal{O}(h^{0.3})$ even with the proposed stabilized method. Combined with the difficulties associated with constructing continuous multiplier fields for embedded interfaces in multiple dimensions (where Γ_*^h is composed of polygonal surfaces), these findings make it difficult to justify pursuing them in the future.

5. SUMMARY AND CONCLUDING REMARKS

In this work, we have examined the use of bubble functions to stabilize a finite element method for imposing Dirichlet constraints on embedded interfaces. We examined a simple model problem that is representative of a much wider class of formulations employing embedded interfaces, including those designed for cohesive crack growth and sharp phase transitions. The challenge is to develop a method that is stable and robust, regardless of the orientation of the interface with respect to the underlying bulk mesh. Previous strategies have approached this problem by redesigning the Lagrange multiplier space or using Nitsche's method. We showed that with a particular choice of basis for the bulk and multiplier fields, bubble-stabilization gives rise to a form that bears strong analogy with Nitsche. The advantage of this approach is that the stabilization parameter follows directly from the choice of bubble enrichment, and the most convenient choice of multiplier can be used. Through several numerical examples, we showed the marked improvement in accuracy in bulk and interfacial fields that follow as a result. We also examined the accuracy of a recently developed domain-integral method. In all cases considered, this technique was shown to provide the most accurate means to evaluate the interfacial flux.

While our findings are promising, we have taken a relatively naive approach in selecting the form of bubble enrichment. Our studies indicate that it may be more advantageous to consider bubble functions that are specifically tailored to the orientation of the interface with respect to the element/mesh. Future work along these lines will consider bubble functions that do not necessarily vanish along element edges. Such edge bubbles might also prove useful for stabilizing penalty methods widely used in the computational mechanics community for more classical, fitted finite element methods.

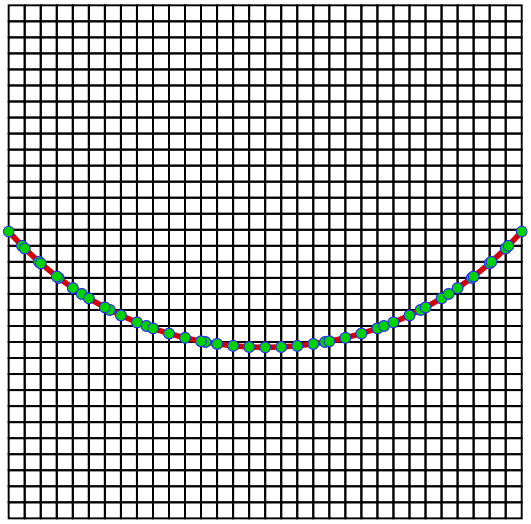

Figure 14. Structured mesh consisting of four-node quadrilateral elements and interfacial mesh. Here the interface Γ_* is a circular arc centered at $(0.5, 1)$, with radius $r = 2/3$.

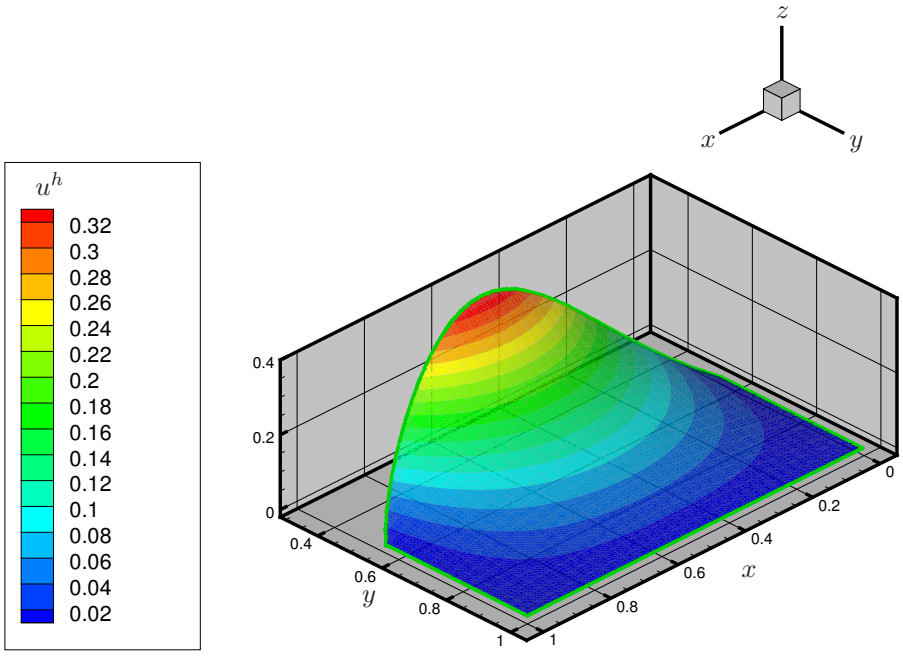

Figure 15. Contour plot of finite-element solution $u^h = \bar{u} + u'$ for the case with a circular interface. These results were obtained on the uniform mesh of quadrilateral elements shown in Figure 14.

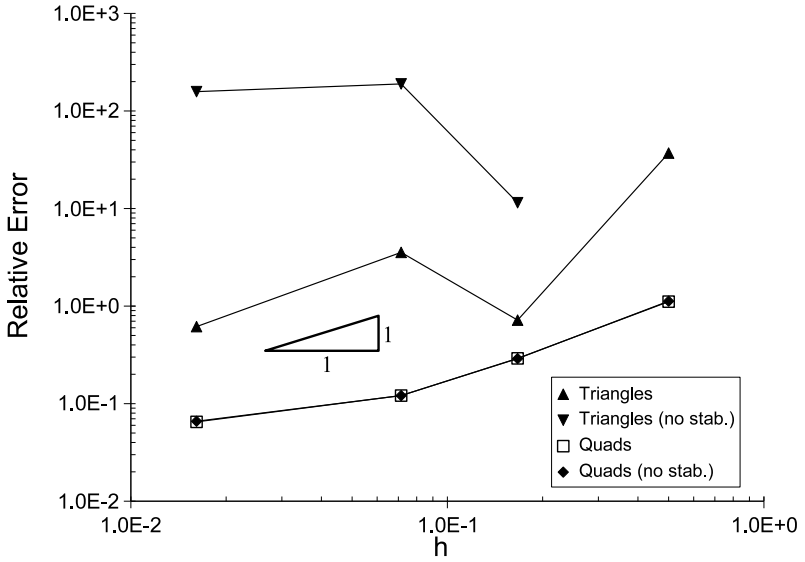

Figure 16. Convergence study results for triangular and quadrilateral grids with circular interface. All results shown pertain to the Lagrange multiplier field.

ACKNOWLEDGEMENTS

The support of Duke University through Sandia National Laboratories grant 184592 is gratefully acknowledged.

REFERENCES

1. Zhang LT, Gerstenberger A, Wang X, Liu WK. Immersed finite element method. *Computer Methods in Applied Mechanics and Engineering* 2004; **193**:2051–2067.
2. Moës N, Belytschko T. Extended finite element method for cohesive crack growth. *Engineering Fracture Mechanics* 2002; **69**(7):813–833.
3. Dolbow JE, Fried E, Ji H. A numerical strategy for investigating the kinetic response of stimulus-responsive hydrogels. *Computer Methods in Applied Mechanics and Engineering* 2005; **194**:4447–4480.
4. Babuška I. The finite element method with Lagrangian multipliers. *Numerische Mathematik* 1973; **20**(3):179–192.
5. Barbosa HJC, Hughes TJR. The finite element method with Lagrange multipliers on the boundary: Circumventing the Babuška-Brezzi condition. *Computer Methods in Applied Mechanics and Engineering* 1991; **85**(1):109–128.
6. Stenberg R. On some techniques for approximating boundary conditions in the finite element method. *Journal of Computational and Applied Mathematics* 1995; **63**:139–148.
7. Nitsche JA. Über ein Variationsprinzip zur Lösung von Dirichlet-Problemen bei Verwendung von Teilräumen, die keinen Randbedingungen unterworfen sind. *Abhandlungen aus dem Mathematischen Seminar der Universität Hamburg* 1970/71; **36**:9–15.
8. Fernandez-Mendez S, Huerta A. Imposing essential boundary conditions in mesh-free methods. *Computer Methods in Applied Mechanics and Engineering* 2004; **193**:1257–1275.
9. Hansbo A, Hansbo P. An unfitted finite element method, based on Nitsche's method, for elliptic interface problems. *Computer Methods in Applied Mechanics and Engineering* 2002; **191**:5537–5552.

10. Ji H, Dolbow JE. On strategies for enforcing interfacial constraints and evaluating jump conditions with the extended finite element method. *International Journal for Numerical Methods in Engineering* 2004; **61**(14):2508–2535.
11. Moës N, Bechet E, Tourbier M. Imposing essential boundary conditions in the extended finite element method. *International Journal for Numerical Methods in Engineering* 2006; Accepted for publication.
12. Belytschko T, Black T. Elastic crack growth in finite elements with minimal remeshing. *International Journal for Numerical Methods in Engineering* 1999; **45**(5):601–620.
13. Hughes, TJR. Multiscale phenomena: Green's functions, the Dirichlet-to-Neumann formulation, subgrid scale models, bubbles and the origins of stabilized methods. *Computer Methods in Applied Mechanics and Engineering* 1995; **127**:387–401.
14. Hughes TJR, Feijóo GR, Mazzei L, Quincy J-B. The variational multiscale method—a paradigm for computational mechanics. *Computer Methods in Applied Mechanics and Engineering* 1998; **166**:3–24.
15. Brezzi F, Bristeau MO, Franca LP, Mallet M, Rogé G. A relationship between stabilized finite element methods and the Galerkin method with bubble functions. *Computer Methods in Applied Mechanics and Engineering* 1992; **96**:117–129.
16. Arnold DN, Brezzi F, Fortin M. A stable finite element for the Stokes equations. *Calcolo* 1984; **21**(4):337–344.
17. Brezzi F, Russo A. Choosing bubbles for advection-diffusion problems. *Mathematical Models and Methods in Applied Sciences* 1994; **4**(4):571–587.
18. Franca LP, Farhat C. Bubble functions prompt unusual stabilized finite element methods. *Computer Methods in Applied Mechanics and Engineering* 1995; **123**:299–308.
19. Brezzi F, Franca LP, Russo A. Further considerations on residual-free bubbles for advective-diffusive equations. *Computer Methods in Applied Mechanics and Engineering* 1998; **166**:25–33.
20. Franca LP, Farhat C, Macedo AP, Lesoinne M. Residual-free bubbles for the Helmholtz equation. *International Journal for Numerical Methods in Engineering* 1997; **40**(21):4003–4009.
21. Franca LP, Nesliturk A, Stynes M. On the stability of residual-free bubbles for convection-diffusion problems and their approximation by a two-level finite element method. *Computer Methods in Applied Mechanics and Engineering* 1998; **166**:35–49.
22. Barbone PE, Harari I. Nearly H^1-optimal finite element methods. *Computer Methods in Applied Mechanics and Engineering* 2001; **190**:5679–5690.
23. Brezzi F, Franca LP, Hughes TJR, Russo A. $b = \int g$. *Computer Methods in Applied Mechanics and Engineering* 1997; **145**:329–339.
24. Franca LP, Madureira AL, Valentin F. Towards multiscale functions: Enriching finite element spaces with local but not bubble-like functions. *Computer Methods in Applied Mechanics and Engineering* 2005; **194**:3006–3021.
25. Hou TY, Wu XH. A multiscale finite element method for elliptic problems in composite materials and porous media. *Journal of Computational Physics* 1997; **134**(1):169–189.
26. Hughes TJR, Sangalli G. Variational multiscale analysis: The fine-scale Green's function, projection, optimization, localization, and stabilized methods. *Institute for Computational Engineering and Sciences (ICES) Report 05-46*; The University of Texas: Austin, November 2005.
27. Pitkäranta J. Boundary subspaces for the finite element method with Lagrange multipliers. *Numerische Mathematik* 1979; **33**(3):273–289.
28. Dahmen W, Kunoth A. Appending boundary conditions by Lagrange multipliers: analysis of the LBB condition. *Numerische Mathematik* 2001; **88**(1):9–42.
29. Daux C, Moës N, Dolbow J, Sukumar N, Belytschko T. Arbitrary branched and intersecting cracks with the extended finite element method. *International Journal for Numerical Methods in Engineering* 2000; **48**(12):1741–1760.
30. Masud A, Khurram RA. A multiscale finite element method for the incompressible Navier-Stokes equations. *Computer Methods in Applied Mechanics and Engineering*; in press.
31. Brezzi F, Marini D, Russo A. Applications of the pseudo residual-free bubbles to the stabilization of convection-diffusion problems. *Computer Methods in Applied Mechanics and Engineering* 1998; **166**:51–63.
32. Carey GF, Chow SS, Seager MK. Approximate boundary-flux calculations. *Computer Methods in Applied Mechanics and Engineering* 1985; **50**(2):107–120.
33. Pehlivanov AI, Lazarov RD, Carey GF, Chow SS. Superconvergence analysis of approximate boundary-flux calculations. *Numerische Mathematik* 1992; **63**(4):483–501.
34. Wagner Gj, Liu WK. Hierarchical enrichment for bridging scales and mesh-free boundary conditions. *International Journal for Numerical Methods in Engineering* 2001; **50**(3):507–524.